ISSN 0023-1584, Kinetics and Catalysis, 2008, Vol. 49, No. 2, pp. 291–298. © MAIK "Nauka/Interperiodica" (Russia), 2008.
Original Russian Text © V.N. Snytnikov, V.O. Stoyanovskii, T.V. Larina, O.P. Krivoruchko, V.A. Ushakov, V.N. Parmon, 2008, published in Kinetika i Kataliz, 2008, Vol. 49, No. 2, pp. 307–314.

Laser-Induced Luminescence of Model Fe/Al_2O_3 and Cr/Al_2O_3 Catalysts

V. N. Snytnikov, V. O. Stoyanovskii, T. V. Larina, O. P. Krivoruchko, V. A. Ushakov, and V. N. Parmon

Boreskov Institute of Catalysis, Siberian Branch, Russian Academy of Sciences, Novosibirsk, 630090 Russia
e-mail: snyt@catalysis.nsk.su

Received November 27, 2006

Abstract—The laser-induced luminescence of Cr^{3+} impurity ions in model Fe/Al_2O_3 and Cr/Al_2O_3 catalysts with different calcination temperatures was studied. It was found that an additional luminescence band at 770 nm appeared in the luminescence spectra of low-temperature samples as a result of the interaction of octahedrally coordinated Cr^{3+} ions with Fe^{3+} impurity ions. In the θ-Al_2O_3 phase with a concentration of Cr^{3+} ions higher than 0.1 wt %, the interaction of the Cr^{3+}–Cr^{3+} ion pairs in the immediate surroundings resulted in the appearance of N_θ lines due to the splitting of R_θ lines. The differences of these lines from the N_α lines of α-Al_2O_3 were related to the individuality of the crystal lattice of the θ phase and the coordination of Cr^{3+} impurity ions in the immediate surroundings, which is different from that in the α phase. Based on the laser-induced luminescence spectroscopic data, it was found that regions with a local Cr^{3+} concentration higher than the average Cr^{3+} concentration in the bulk of a catalyst by one order of magnitude were formed in the α-Al_2O_3–Fe_2O_3 system with the bulk Fe and Cr concentrations of 2.5 and 0.04 wt %, respectively, which was calcined at 1220°C, as a result of the diffusion of chromium and iron ions.

DOI: 10.1134/S0023158408020183

INTRODUCTION

Many catalysts for the dehydrogenation of light alkanes have been developed based on Al_2O_3 as a support and the oxides of transition metals (such as Fe and Cr) as active components [1, 2]. The properties of the active centers of these systems depend on the interaction of transition metal ions with Al_2O_3 and, probably, impurities, which inevitably occurred in real samples. Laser-induced luminescence is one of a few optical techniques for the detection of low impurity concentrations and the bulk states of ions in heterogeneous systems [3]. Snytnikov et al. [4] studied the luminescence of a number of catalysts and Al_2O_3 as a support with trace amounts of chromium, iron, manganese, etc. It was found that the phase and elemental compositions of a thin surface layer, as well as the temperature of this layer under conditions of real pressures and gas atmospheres, can be determined from the laser-induced luminescence spectra using the characteristic luminescence lines of Cr^{3+} ions for α- and θ-alumina phases. The appearance of the octahedrally coordinated Cr^{3+} impurity ions of corundum in metastable alumina forms was detected using luminescence excited by UV radiation from an ArF laser with a wavelength of 193 nm with a sensitivity of no worse than 10^{-7} wt %. Snytnikov et al. [5] found the single-photon mode of the action of pulsed radiation from an ArF laser on the samples of Al_2O_3 for luminescence.

The aim of this work was to study the pair interaction of Fe–Cr and Cr–Cr centers in model Fe/Al_2O_3 and Cr/Al_2O_3 catalysts using laser-induced luminescence at transition metal concentrations of no higher than 2.5 wt %.

EXPERIMENTAL

The pseudoboehmite powder, which was prepared by spraying a suspension in a drier at an outlet temperature of 110°C, was mixed with a specified amount of powdered $Cr(NO_3)_3 \cdot 9H_2O$ or $Fe(NO_3)_3 \cdot 9H_2O$ of analytical grade in a laboratory mixer; then, the contents were wetted with distilled water acidified to pH 2.0. In this case, pastes with a 55 wt % moisture content were obtained; rings with the diameters d_{outer} = 15 mm and d_{inner} = 4 mm and 15 mm in height were formed from these pastes. These rings were dried at room temperature for 72 h and then calcined in a muffle furnace at 750, 970, and 1220°C for 8 h. The study was performed with powder samples prepared by crushing the rings. In addition, a ruby single crystal (Cr^{3+} in α-Al_2O_3) was used for comparing absorption spectra [4].

The laser-induced luminescence experiments were performed on a spectroscopic bench at the Boreskov Institute of Catalysis, Siberian Branch of the Russian Academy of Sciences. This bench and the experimental procedure were described elsewhere [3, 4]. The spectra

Table 1. Characteristics of the test samples of Al_2O_3

Sample no.	Sample composition	Temperature*, °C	Phase composition of samples according to XRD data
1	Al_2O_3	750	A mixture of γ-Al_2O_3 and χ-Al_2O_3 (no more than 15%)
2	0.1% Cr/Al_2O_3		Lattice parameter a = 7.920 Å
3	0.5% Cr/Al_2O_3		
4	2.5% Cr/Al_2O_3		
5	0.1% Fe/Al_2O_3		
6	0.5% Fe/Al_2O_3		
7	2.5% Fe/Al_2O_3		
8	Al_2O_3	970	A mixture of δ-Al_2O_3 and trace α-Al_2O_3 (H_{43} = 5**)
9	0.1% Cr/Al_2O_3	970	A mixture of δ-Al_2O_3 and trace α-Al_2O_3 (H_{43} = 8)
10	0.5% Cr/Al_2O_3	970	A mixture of δ-Al_2O_3 and trace α-Al_2O_3–α-Cr_2O_3 solid solution based on the α-Al_2O_3 structure
11	2.5% Cr/Al_2O_3	970	Diffraction pattern from θ-Al_2O_3; The α-Al_2O_3 phase was not detected
12	0.1% Fe/Al_2O_3	970	Diffraction pattern from δ-Al_2O_3; The α-Al_2O_3 phase was not detected
13	0.5% Fe/Al_2O_3	970	A mixture of δ-Al_2O_3 and trace α-Al_2O_3 (H_{43} = 10)
14	2.5% Fe/Al_2O_3	970	A mixture of δ-Al_2O_3 and trace α-Al_2O_3 (H_{43} = 90)
15	Al_2O_3	1220	δ-Al_2O_3 (d/n_{024} = 1.7319 Å)
16	0.1% Cr/Al_2O_3	1220	α-Al_2O_3–α-Cr_2O_3 solid solution based on the α-Al_2O_3 structure (a wide range of solutions with averaged d/n_{024} = 1.7362 Å)
17	0.5% Cr/Al_2O_3	1220	α-Al_2O_3–α-Cr_2O_3 solid solution based on the α-Al_2O_3 structure (d/n_{024} = 1.7393 Å)
18	2.5% Cr/Al_2O_3	1220	α-Al_2O_3–α-Cr_2O_3 solid solution based on the α-Al_2O_3 structure (d/n_{024} = 1.7411 Å)
19	0.1% Fe/Al_2O_3	1220	α-Al_2O_3–Fe_2O_3 solid solution based on the α-Al_2O_3 structure (a wide range of solutions with averaged d/n_{024} = 1.7405 Å)
20	0.5% Fe/Al_2O_3	1220	α-Al_2O_3–Fe_2O_3 solid solution based on the α-Al_2O_3 structure (a wide range of solutions with averaged d/n_{024} = 1.7380 Å)
21	2.5% Fe/Al_2O_3	1220	α-Al_2O_3–Fe_2O_3 solid solution based on the α-Al_2O_3 structure (a wide range of solutions with averaged d/n_{024} = 1.7436 Å)

*The time of sample calcination at the specified temperature was 5 h.

**Peak intensity.

were excited using an ArF laser (λ = 193 nm) with the pulse duration τ_p = 15 ns and a radiation power density of no higher than 0.1 MW/cm^2 at the sample surface (the heating of an absorbing layer was insignificant at this power density) [5]. The laser-induced luminescence spectrum was measured with an MDR-12 high-aperture monochromator (LOMO, Russia) and an LN/CCD-1100PF/UV spectroscopic chamber (Princeton Instruments, United States) with the spectral sensitivity range 180–900 nm.

The analysis of samples for impurities was performed on a SPRUT-001 X-ray fluorescence spectrometry analyzer (Russia). The X-ray diffraction (XRD) analysis of samples was performed on URD-63 and HZG-4 diffractometers (Germany) using CuK_α radiation. The electronic diffuse reflectance spectra were measured on a UV–VIS 4501 instrument (Shimadzu, Japan).

RESULTS

Table 1 summarizes the characteristics (composition, calcination temperature, and XRD data) of the test samples.

According to X-ray fluorescence spectrometric data, the starting hydroxides, which were used for preparing alumina, contained the following impurities (wt %): Si, 0.57; Fe, 0.05; Cr, 0.01; Mn, 0.01; Na, <0.01. The concentration of other impurities was no higher than 0.001 wt %. In the samples doped with Fe to a concentration of 2.5 wt %, increased Cr and Mn impurity concentrations of 0.04 and 0.005 wt %, respectively, were detected (Table 2).

XRD analysis allowed us to detect an α-Al_2O_3 phase in the bulk of the samples with a sensitivity of a few wt %. Changes in the oxide lattice of Al_2O_3 upon doping with Cr and Fe and the formation of solid solutions like Cr_2O_3–Al_2O_3 and Fe_2O_3–Al_2O_3 based on the α-Al_2O_3 structure were also monitored using XRD

analysis. The sets of interplanar spacings in δ- and θ-Al_2O_3 phases are similar; because of this, the sensitivity of XRD analysis in the quantitative determination of either of these individual phases was no higher than 20% (Table 1) [6].

The diffuse reflectance UV–VIS spectra of electron transitions allowed us to determine the concentration and coordination of the main doping elements. Figure 1 shows the electronic diffuse reflectance spectra of samples 4, 11, and 18 with a Cr content of 2.5 wt %; the absorption spectrum of a ruby single crystal; and the diffuse reflectance spectra of samples 7, 14, and 21 with a Fe content of 2.5 wt % with various calcination temperatures.

The laser-induced luminescence observed in the test samples was due to the radiative transitions of photoexcited octahedrally coordinated Cr^{3+} ions in the lattice of Al_2O_3. As the concentration of chromium in the samples was increased up to 0.5 wt %, the luminescence intensity at *R* lines, which are characteristic of Cr^{3+} in α- and θ-Al_2O_3 phases, and a diffuse luminescence band, which is characteristic of low-temperature Al_2O_3 phases, increased. As the doping impurity concentration was further increased, the luminescence intensity decreased. This is consistent with the well-known concentration quenching of the R_α luminescence lines of Cr^{3+} in corundum at a concentration of higher than 0.15 wt % [7]. The introduction of Fe^{3+} ions into the lattice of Al_2O_3 in the iron doping of the samples with concentrations to 2.5 wt % resulted in the luminescence quenching of Cr^{3+} centers.

1. Samples with a Calcination Temperature of 750°C

According to XRD data, samples 1–7 (Table 1), which were calcined at 750°C, were mixtures of γ-Al_2O_3, which is characteristic of the pseudoboehmite series with the lattice parameter a = 7.920 Å, and χ-Al_2O_3 (the concentration of the latter phase was no higher than 15%). The presence of other crystallized phases was not detected.

The electronic diffuse reflectance spectra of chromium-doped samples (Fig. 1, sample 4) exhibited intense lines at 27000 cm^{-1}. According to published data [2, 8], these lines correspond to Cr^{6+} surface sites ($\mathbf{Cr_s^{6+}}$) with an $O^{2-} \longrightarrow Cr^{6+}$ ligand–metal charge-transfer (LMCT) band at 37000 cm^{-1}. In addition to these lines, lower intensity lines at 16600 and 21700 cm^{-1}, which are ascribed to *d–d* transitions in Cr^{3+} surface sites ($\mathbf{Cr_s^{3+}}$), and weak lines at 14600, 17800, and 24700 cm^{-1} due to *d–d* transitions in octahedrally coordinated Cr^{3+} ions in the lattice of Al_2O_3 can also be seen. The intensity of the above bands increased with chromium content. The exception is provided by lines at 27000 and 37000 cm^{-1}, whose

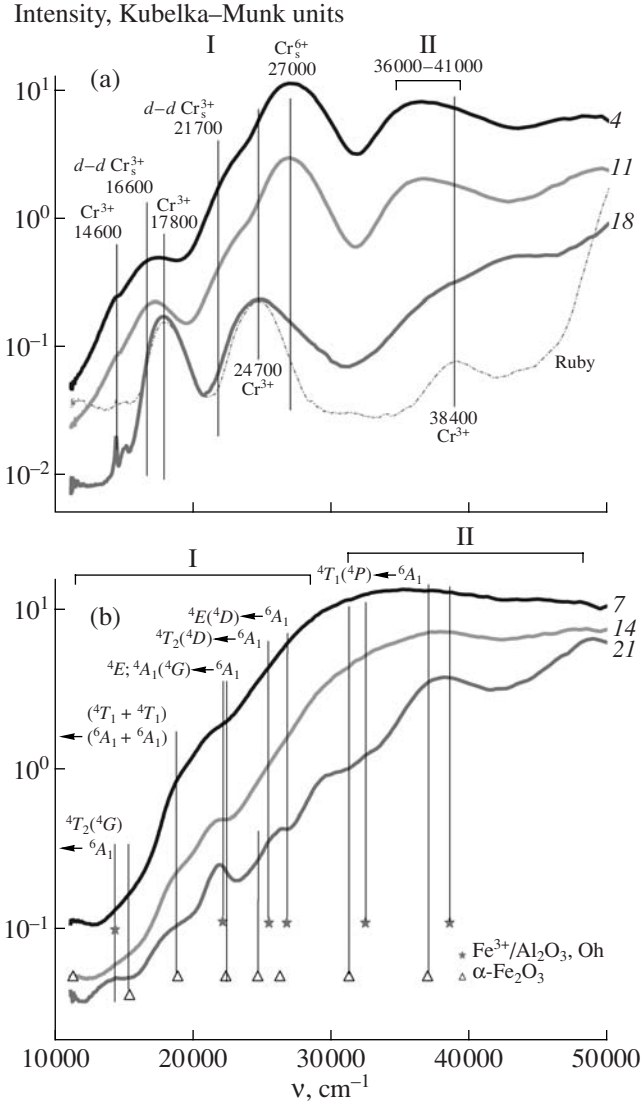

Fig. 1. Electronic diffuse reflectance spectra of (a) samples 4, 11, and 18 containing 2.5% Cr and (b) samples 7, 14, and 21 containing 2.5% Fe and (a) the absorption spectrum of a ruby single crystal (see Table 1 for sample numbers and calcination temperatures): (*I*) region of *d–d* transitions and (*II*) region of (a) Cr^{6+}–O and (b) Fe(III)–O charge-transfer bands.

intensities began to reach saturation at a 0.5 wt % chromium content of the sample.

The iron-doped samples (Table 1, sample 7) exhibited intense LMCT bands due to ligand–metal (Fe^{3+}) charge transfer at wavelengths longer than 30000 cm^{-1}. In addition, lines due to $^4T_2(^4G) \longleftarrow {}^6A_1$ *d–d* transitions at 14000 cm^{-1} and $(^4E; {}^4A_1) \longleftarrow {}^6A_1$ *d–d* transitions at 22300 cm^{-1} and a line at 18500 cm^{-1}, which corresponds to the $(^4T_1 + {}^4T_1) \longleftarrow (^6A_1 + {}^6A_1)$ electron pair transition (EPT) for α-Fe_2O_3, were observed [9]. The samples with an Fe content of 0.1 wt % exhibited lines

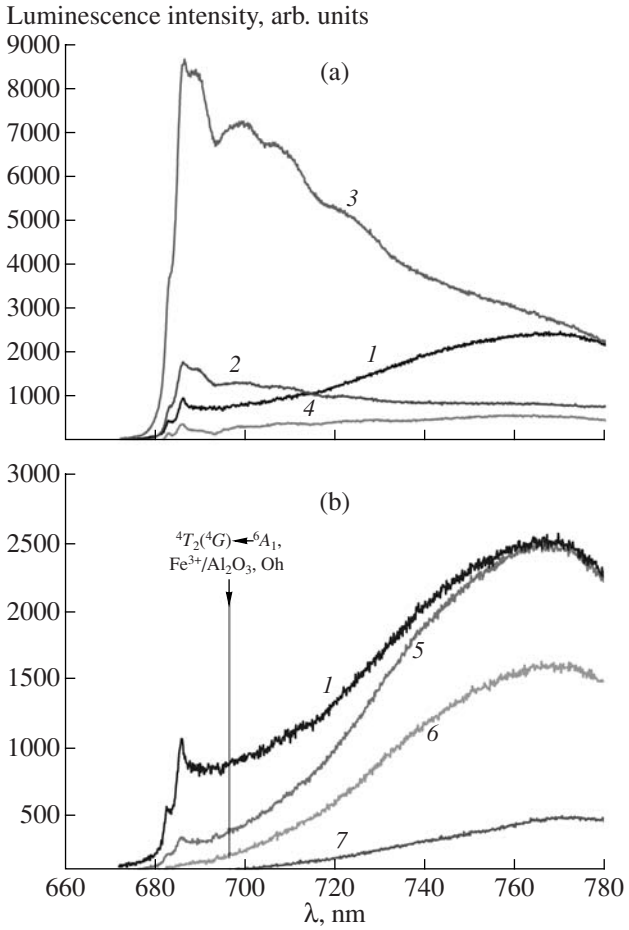

Fig. 2. Luminescence spectra of γ-Al_2O_3 samples doped with (a) Cr and (b) Fe. Sample temperature, 77 K (see Table 1 for sample numbers and composition).

at 27000 and 37000 cm^{-1} from Cr_s^{6+} ions and weak bands from Cr^{3+} in the wavelength regions 16500–18000 and 21000–23000 cm^{-1}.

The laser-induced luminescence spectra of sample 1 with an initial Cr concentration of 0.01 wt % and chromium-doped samples 2–4 exhibited a broad luminescence band with a band head at 680 nm (Fig. 2), which corresponds to the broadened R_θ lines of a θ-Al_2O_3 phase [4]. The luminescence intensity of the chromium-doped samples decreased towards long wavelengths up to $\lambda \approx 1000$ nm. In samples 5–7, which were doped with Fe^{3+} ions, an increase in the concentration of iron resulted in the luminescence quenching of Cr^{3+} primarily at a band at 680–730 nm and, consequently, in the formation of a luminescence maximum at 770 nm.

2. Samples with a Calcination Temperature of 970°C

According to XRD data (Fig. 3), samples 8–14 (Table 1), which were calcined at 970°C, were mixtures of a predominant δ-Al_2O_3 phase and α-Al_2O_3 phase

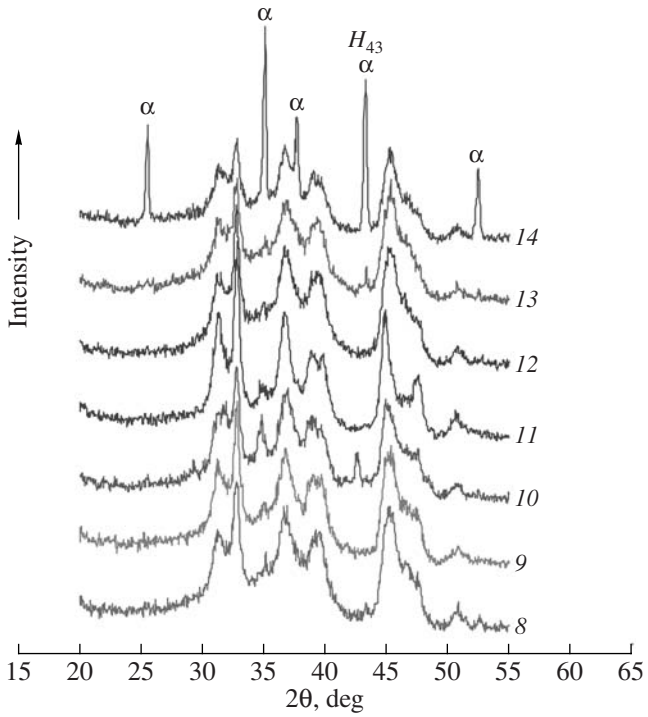

Fig. 3. X-ray diffraction patterns of samples 8–14 calcined at 970°C over the angle range $2\theta = 20°$–55°. α refers to lines that correspond to α-Al_2O_3 (see Table 1 for sample numbers and calcination temperatures).

traces. Only samples 11 (2.5% Cr/Al_2O_3) and 12 (0.1% Fe/Al_2O_3) consisted of a θ-Al_2O_3 phase without the detectable presence of α-Al_2O_3. From a comparison of H_{43} peak intensities, it follows that samples 13 and 14 containing 0.5 and 2.5 wt % Fe, respectively, were characterized by the highest α-Al_2O_3 contents (Table 1). It is believed that an increase in the concentration of iron facilitated the formation of α-Al_2O_3.

As compared with the electronic diffuse reflectance spectra of samples 1–7 (calcination temperature of 750°C), the spectra of samples 8–14 (calcination temperature of 750°C) were characterized by lower absorbance over the entire spectral range with the retention of characteristic lines (Fig. 1, spectra *11* and *14*).

The laser-induced luminescence spectra of samples 8–14 (Fig. 4) exhibited the R_α lines of α-Al_2O_3 at 693.5 and 692.0 nm (marked as R_α in Fig. 4) against the background of a diffuse band characteristic of low-temperature Al_2O_3 phases except for samples 11 (2.5% Cr/Al_2O_3) and 12 (0.1% Fe/Al_2O_3), which did not contain the α phase according to XRD data. Intense R_θ luminescence lines at 682.6 and 685.9 nm, which suggested the presence of θ-Al_2O_3 in the samples, were detected in all of the above samples. In this sample series, the intensities of R_α and R_θ lines were near the threshold of sensitivity at the used excitation level and CCD detector exposure only for sample 14 (2.5% Fe/Al_2O_3) with the highest α-phase content (according to XRD data).

In the series of samples 8–11, both the intensity of a diffuse band and the intensities of R_θ lines increased as the chromium content of the samples was increased up to 0.1 wt % followed by a decrease in the luminescence intensity as the Cr content of the samples was further increased to 2.5 wt %. As the Fe concentration was increased from 0.05 to 2.5 wt % in the series of samples 8 and 12–14, the quenching of R_θ luminescence lines occurred.

In addition to the well-known R_α and R_θ lines, the luminescence spectra of samples 9–11 with Cr contents higher than 0.1 wt % exhibited a number of new lines in the region 688.5–711.0 nm (Fig. 4). An intense line at 696.6 nm was detected in sample 11 (2.5% Cr/Al_2O_3) with a maximum Cr^{3+} content; the presence of α-Al_2O_3 in this sample was not detected using the above techniques.

3. Samples with a Calcination Temperature of 1220°C

According to XRD data, α-Al_2O_3 was formed in sample 15 (i.e., Al_2O_3 with initial background Cr and Fe concentrations) at a calcination temperature of 1220°C. In samples 16–21, solid solutions based on the α-Al_2O_3 were formed: Al_2O_3–Cr_2O_3 (samples 16–18) and Al_2O_3–Fe_2O_3 (samples 19–21). Upon the introduction of Cr^{3+} or Fe^{3+} ions into the lattice of Al_2O_3, the replacement of the Al^{3+} ion by bulkier cations resulted in an increase in interatomic distances; because of this, the positions of XRD lines shifted toward increased lattice parameters. Thus, for a pure α-Cr_2O_3 phase, the position of the 024 line corresponds to d/n_{024} = 1.8152 Å, and d/n_{024} = 1.8406 Å for α-Fe_2O_3. The line positions for the samples of an α-Al_2O_3 phase with Cr and Fe concentrations to 0.5 wt % are inconsistent with the value of d/n_{024} = 1.7400 Å given in an XRD database [10]. This can be indirect evidence for the incomplete formation of an α-alumina phase at low concentrations of dopant ions.

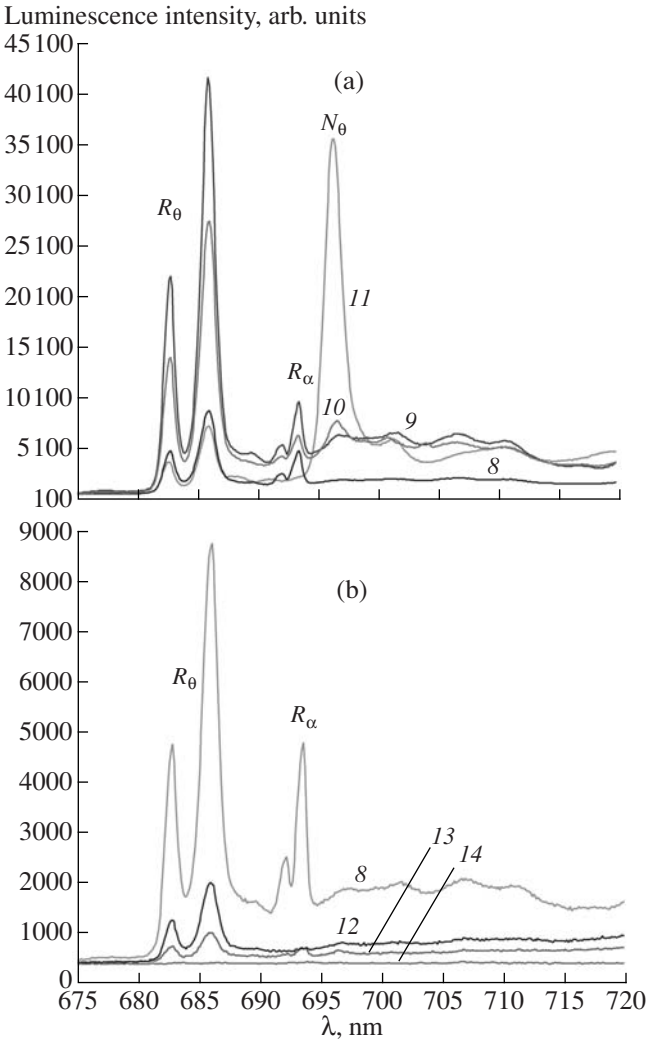

Fig. 4. Luminescence spectra of samples 8–14 doped with (a) Cr and (b) Fe and calcined at 970°C. Sample temperature, 77 K (see Table 1 for sample numbers and composition).

The electronic diffuse reflectance spectra of chromium-doped samples are indicative of the almost complete disappearance of absorption bands at 27000 and 37000 cm^{-1} due to surface Cr_s^{6+} ions. The Cr^{3+} sites, which are characterized by bands at 14600, 17800, and 24700 cm^{-1}, were predominant in the samples. It is likely that a small amount of surface Cr_s^{3+} sites with characteristic bands at 16600 and 21700 cm^{-1} occurred (Fig. 1, sample 18). Upon the addition of iron, the Fe(III)–O and Fe–O LMCT bands at 38600 and 40000 cm^{-1}, respectively; the Fe^{3+}–Fe^{3+} $({}^4T_1 + {}^4T_1) \leftarrow ({}^6A_1 + {}^6A_1)$ EPT bands at 18500 cm^{-1} for α-Fe_2O_3; and an intense narrow line at 22300 cm^{-1} due to the $({}^4E; {}^4A_1) \leftarrow {}^6A_1$ transition in Fe^{3+} were observed. The intensity of the above bands increased with iron content of the samples. In the samples containing 0.1 wt % Fe, bands at 17 800 and 24 700 cm^{-1} were prominent; they corresponded to the Cr^{3+} sites formed from impurities.

The luminescence spectra of chromium-doped Al_2O_3 samples 15–21 exhibited intense R_α lines due to Cr^{3+} and a band due to vibronic transitions at 705–715 nm, which is characteristic of ruby (Fig. 5, sample 19) [11]. The concentration quenching of luminescence at R_α lines came into play at chromium concentrations higher than 0.1 wt %. Moreover, the laser-induced luminescence spectra of samples 16–19 at 77 K usually exhibited R lines due to Mn^{4+} impurity ions, whose concentration was 0.01 wt % (Table 2) [4] and the R-doublet splitting was $\Delta\nu$ = 80 cm^{-1}.

In addition to the above lines, N_α luminescence lines were detected in samples 16–18 at chromium concentrations higher than 0.1 wt % (Fig. 6). Vink and DeBruin [12] related these lines to the splitting of chro-

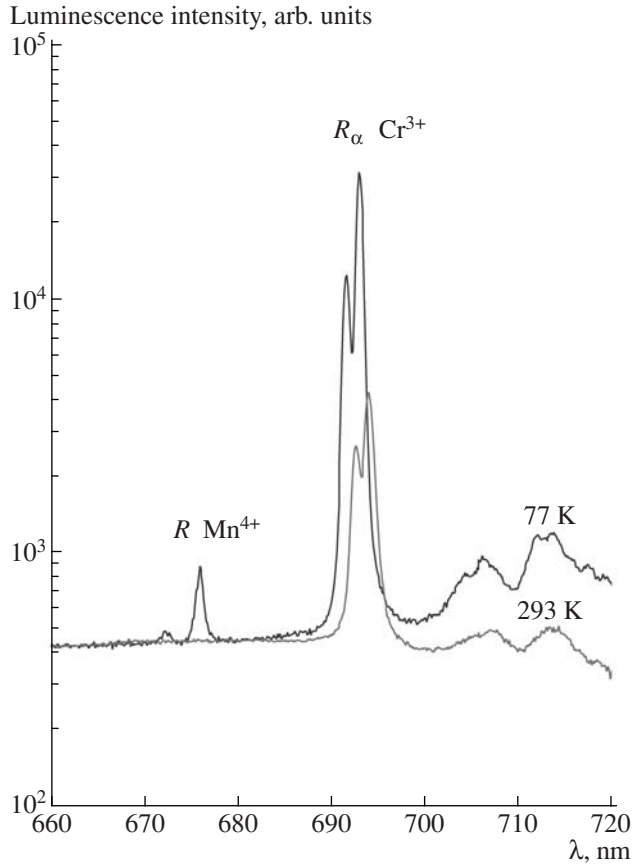

Fig. 5. Laser-induced luminescence of sample 19 (0.1% Fe/Al_2O_3; 1220°C) at 293 and 77 K.

mium R_α lines due to the pair interaction of Cr^{3+}–Cr^{3+} ions from the immediate surroundings. We detected the quenching of N_α lines at Cr concentrations in the samples higher than 0.5 wt %; this quenching was due to a concentration effect common to R_α and N_α lines.

Luminescence quenching at the R_α lines of α-Al_2O_3 occurred as the Fe content was increased from 0.05 to 2.5 wt %. Nevertheless, we detected the N_α lines of Cr^{3+} ions in the luminescence spectrum of sample 21 (2.5% Fe/Al_2O_3), unlike the spectra of samples 19 and 20 with

Table 2. Concentrations of impurities in the test samples according to X-ray fluorescence spectrometry

Sample		Impurity concentration, wt %		
no.*	composition	Cr	Mn	Fe
15	Al_2O_3	0.01	0.01	0.05
16	0.1% Cr/Al_2O_3	0.11	0.01	0.05
19	0.1% Fe/Al_2O_3	0.02	0.01	0.15
21	2.5% Fe/Al_2O_3	0.04	0.05	2.30

* Corresponds to the sample number in Table 1.

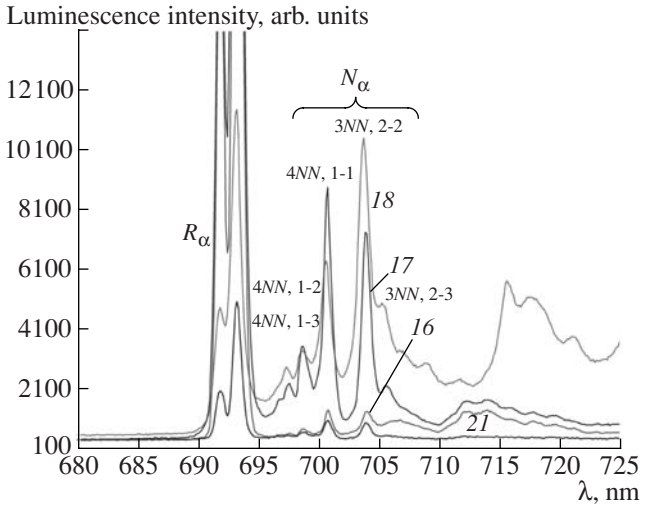

Fig. 6. Luminescence spectra of α-Al_2O_3 samples (T_{calc} = 1220°C) doped with (*16–18*) Cr and (*21*) Fe. Sample temperature, 77 K (see Table 1 for sample composition).

lower Fe contents, in which the above lines were not detected.

DISCUSSION

The radiative transitions of the photoexcited d^3 electrons of octahedrally coordinated Cr^{3+} impurity ions in the most ordered α- and θ-alumina phases were responsible for luminescence R lines. The R_α and R_θ line positions coincide with the position found previously [3, 4] for samples with trace concentrations of Cr^{3+} impurity ions in aluminum oxide. A broad diffuse luminescence band with a band head corresponding to the broadened R_θ lines of a θ phase and the absence of intense lines from the spectra of γ-, χ-, and δ-Al_2O_3 were due to the strong disordering of the crystal lattices of the above phases. The presence of hydroxyl groups (OH^-) in the first coordination sphere of the Cr^{3+} impurity ion can also have a certain effect.

The R-line luminescence intensity (I_{Cr}) at 685.9–693.5 nm in samples 1–4 was related to the chromium content by the expression $I_{Cr} \sim [Cr]^{0.5}$. As the Fe content of the samples was increased from 0.05 to 2.5 wt %, the character of Cr^{3+} luminescence quenching depended on the luminescence wavelength. Thus, the intensity of Cr^{3+} R lines at 682–695 nm depended on the Fe concentration in accordance with the law $I_{Cr}(682–695) \sim [Fe]^{-0.75}$. At the same time, this relationship was close to $I_{Cr}(770) \sim \exp(-[Fe])$ at 770 nm. It is most likely that the high efficiency of Cr^{3+} luminescence quenching in the region of R lines upon doping with iron was related to the $^4T_2(^4G) \longleftarrow {}^6A_1$ transition at 14350 cm^{-1} for octahedrally coordinated Fe^{3+} ions in Al_2O_3. Thus, the observed broad luminescence band with a maximum at 770–800 nm in these samples was a consequence of a

considerable interaction between photoexcited Cr^{3+} and Fe^{3+} impurity ions. This is additional evidence that it is of importance to take into account the interaction of impurity ions even at their trace concentrations.

At a calcination temperature of 970°C, the formation of a δ-Al_2O_3 phase with α-Al_2O_3 traces occurred in the majority of samples (8–10, 13, and 14). In the series of samples 8–11, the intensities of both a diffuse luminescence band and R_θ lines increased as the concentration of chromium was increased up to 0.1 wt % followed by a decrease in the intensity of luminescence as the Cr content of the samples was increased to 2.5 wt %. In the series of samples 8 and 12–14, an increase in the Fe content from 0.05 to 2.5 wt % resulted in a decrease in the R_θ-line luminescence intensity by more than three orders of magnitude. Nevertheless, the concentration of an α-Al_2O_3 phase in the samples with iron ions added, which was calculated from the luminescence intensity of R_α lines using a given relationship for α-Al_2O_3 [3], was consistent with XRD data.

In all of the samples with a calcination temperature of 970°C, intense luminescence lines were detected at 682.6 and 685.9 nm, which suggest the presence of a θ-Al_2O_3 phase in the samples (this phase was not detected by XRD analysis). This discrepancy in conclusions drawn based on the use of various techniques can be due to difficulties in the XRD detection of the θ phase against the background of the δ phase because of the similar sets of interplanar spacings in these phases. At the same time, the θ phase can easily be detected by an intense characteristic doublet of narrow R_θ lines in luminescence spectra. Nevertheless, the question of qualitative differences (line width and position, decay times, etc.) between the luminescence spectra of the δ and θ phases is still an open question. This problem can be solved with the availability of a reference sample of the pure δ-Al_2O_3 phase.

The luminescence spectra of the test samples with calcination temperatures of 970 and 1220°C (Figs. 4–6) exhibited the well-known R_α, R_θ, and N_α lines; in this case, the N_α lines were due to the pair interaction of Cr^{3+}–Cr^{3+} ions. However, new luminescence lines, which were marked as N_θ, were detected in the region 688.5–711.0 nm for samples with a calcination temperature of 970°C and a Cr content of higher than 0.1 wt % (Fig. 4). The intensity of the most intense N_θ lines at 696.7 and 701.4 nm increased with the Cr content of the samples in accordance with a quadratic law (more rapidly than the intensities of R_θ lines). This allowed us to assume that the N_θ lines are due to the pair interaction of Cr^{3+} ions in the θ-Al_2O_3 phase analogously to N_θ lines in corundum. We failed to find published experimental or theoretical data on the splitting of Cr^{3+} R_θ lines in a pure phase of θ-Al_2O_3 because of the pair interaction of Cr^{3+}–Cr^{3+} ions in the immediate surroundings.

The samples with a calcination temperature of 1220°C were characterized by a linear increase in the luminescence intensity of R_α lines as the concentration of Cr was increased up to 0.1 wt %. The intensity of N_α and R_α lines decreased at a Cr content of the samples higher than 0.5 wt %. The intensity ratio between N_α and R_α luminescence lines was found proportional to the concentration of chromium ions in the samples: $I_{N_{1,\alpha}}/I_{R_{2,\alpha}} \sim [Cr]$. This allowed us to determine the local concentration of emitting Cr^{3+} ions from this ratio even in the presence Fe^{3+} ions, which quench the above lines.

We used this opportunity to calculate the local concentration of Cr^{3+} in sample 21 (2.5% Fe/Al_2O_3; 1220°C) with a high Fe content. The Cr^{3+} concentration calculated from the $I_{N_{1,\alpha}}/I_{R_{2,\alpha}}$ ratio measured in laser-induced luminescence spectra was found equal to 0.7 wt %. At the same time, according to X-ray fluorescence analysis, the average chromium content of this sample was equal to 0.04 wt % (Table 2). This considerable increase in the laser-induced luminescence intensity of the sample under discussion can be explained by the ejection of Cr^{3+} ions by Fe^{3+} ions from nanosized domains in α-Al_2O_3, which were formed at high calcination temperatures (1220°C) in the α-Al_2O_3–Fe_2O_3 system, to the boundaries of these nanodomains with the formation of a region with a high (0.7 wt %) local concentration of chromium. This concentration is higher than the average bulk concentration of Cr^{3+} by one order of magnitude. This ejection of impurities to the phase boundary microdomains has been repeatedly observed in cerium oxide [14] and aluminum oxide [15].

In a ruby single crystal at 293 K, the characteristic R_1-line halfwidth was ~11 cm^{-1} and it decreased to 0.12–0.30 cm^{-1} upon cooling the single crystal to 77 K [13]. In this case, the residual R-line halfwidth primarily depended on the occurrence of nonuniform stresses in a crystal and crystal lattice defects. In sample 15 (Al_2O_3) at 293 K, the characteristic R_1-line halfwidth was ~23 cm^{-1}; this line broadened to ~28 cm^{-1} as the concentration of Cr^{3+} was increased. The observed broadening of R_1 and other lines in the test samples of model catalysts can also be due to crystal lattice defects and, probably, an increase in the number of interacting pairs of chromium ions at Cr^{3+} concentrations of higher than 0.5 wt %. The change in the ratio between the line intensities I_{R_1} and I_{R_2} from 1.77 (T = 293 K) for a ruby single crystal and α-Al_2O_3 samples with small Cr and Fe additives to 1.90 (T = 293 K) as the chromium concentration in sample 15 was increased to 2.5 wt % suggests an increase in the number of crystal lattice defects.

CONCLUSIONS

The above study of aluminum oxides doped with chromium and iron supported the assumption that laser-induced luminescence spectra can provide valuable information on the internal structure of catalysts. Thus, the interaction of Cr^{3+} and Fe^{3+} impurity ions in low-temperature γ-, χ-, and δ-Al_2O_3 phases can result in the appearance of an additional luminescence band due to Cr^{3+} ions at 770 nm. At a concentration of Cr^{3+} ions higher than 0.1 wt % in samples containing a θ-Al_2O_3 phase, N_θ lines due to the splitting of R_α lines on the interaction of Cr^{3+}–Cr^{3+} ion pairs in the immediate surroundings were observed. Differences between the N_α lines and the well-known N_α lines in corundum are due to the individuality of the crystal lattice of the θ-Al_2O_3 phase and the coordination of Cr^{3+} impurity ions in the immediate surroundings other than that in the α-Al_2O_3 phase.

The laser-induced luminescence-spectroscopic data indicate that, at an alumina calcination temperature of 1220°C, regions with a local Cr^{3+} concentration higher than the average Cr^{3+} concentration in the bulk of the catalyst by an order of magnitude were formed as a result of the segregation of Cr^{3+} and Fe^{3+} ions in the α-Al_2O_3–Fe_2O_3 system at an iron content of 2.5 wt %. It is believed that this phenomenon was related to the displacement of impurities to the boundaries of the formed nanodomains of a crystalline α-Al_2O_3 phase.

Luminescence line broadening and line intensity ratios at high concentrations of impurity ions can serve as a source of data on not only the phase composition (as found previously [3, 4] for Al_2O_3 with trace concentrations of Cr^{3+} impurity ions) but also the quantitative values of parameters that characterize the formation and defect structure of the crystal lattices of catalysts based on Al_2O_3.

Considerable differences in the positions of *R* and *N* luminescence lines, which are characteristic of octahedrally coordinated Cr^{3+} ions in the lattices of α- and θ-alumina phases, allowed us to use laser-induced luminescence spectra for the determination of the phase composition of a thin surface layer and the elemental composition in the microstructure studies of real heterogeneous catalysts, in particular, under in situ conditions at real pressure and gas atmosphere composition. Studies of a commercial chromium-containing dehydrogenation catalyst (OAO Katalizator), whose composition is more complex than that of the model test samples, are currently in progress.

ACKNOWLEDGMENTS

This work was supported in part by the "Support to Leading Scientific Schools" program (grant no. NSh-1484-2003.3). We are grateful to G.M. Zhidomirov for critical comments and helpful discussions.

REFERENCES

1. Gorriz, O.F. and Cadus, L.E., *Appl. Catal., A*, 1999, vol. 180, p. 247.
2. Puurunen, R.L. and Weckhuysen, B.M., *J. Catal.*, 2002, vol. 210, p. 418.
3. Snytnikov, V.N., Stoyanovskii, V.O., Raspopin, K.S., and Parmon, V.N., *Dokl. Akad. Nauk*, 2003, vol. 392, p. 501 [*Dokl. Phys. Chem.* (Engl. Transl.), vol. 392, p. 259].
4. Snytnikov, V.N., Stoyanovskii, V.O., Ushakov, V.A., and Parmon, V.N., *Kinet. Katal.*, 2005, vol. 46, no. 2, p. 278 [*Kinet. Catal.* (Engl. Transl.), vol. 46, no. 2, p. 260].
5. Snytnikov, V.N., Stoyanovskii, V.O., Rudina, N.A., and Parmon, V.N., *Zh. Tekh. Fiz.*, 2006, vol. 76, p. 124.
6. Ushakov, V.A. and Moroz, E.M., *Kinet. Katal.*, 1985, vol. 26, p. 963.
7. Gevorkyan, V.A., Madatyan, K.A., Kochinyan, E.A., et al., *Spektroskopiya kristallov* (Spectroscopy of Crystals), Moscow: Nauka, 1970.
8. Weckhuysen, B.M., Schoofs, B., and Schoonheydt, R.A., *J. Chem. Soc., Faraday Trans.*, 1997, vol. 93, no. 11, p. 2117.
9. Sherman, D.M., *Phys. Chem. Minerals*, 1985, vol. 12, p. 161.
10. PC-ICDD PDF-2.
11. Nelson, D.F. and Sturge, M.D., *Phys. Rev. A*, 1965, vol. 137, no. 4, p. 1117.
12. Vink, A.P. and DeBruin, M.A., *J. Phys.: Condens. Matter*, 2000, vol. 12, p. 8607.
13. Morgenshtern, Z.L. and Nevstruev, V.V., *Opt. Spektrosk.*, 1966, vol. 20, p. 837.
14. Borchert, H. and Frolova, Y.V., *J. Phys. Chem. B*, 2005, vol. 109, p. 5728.
15. Kebbede, A. and Carim, A.H., *Mater. Lett.*, 1999, vol. 41, p. 198.